Sustainable Production and Consumption 51 (2024) 657–669

Contents lists available at ScienceDirect

Sustainable Production and Consumption

journal homepage: www.elsevier.com/locate/spc

A sustainability analysis for a circular power-to-liquid process for diesel production

Grazia Leonzio [a,b,*], Niki Triantafyllou [b], Nilay Shah [b]

[a] Cagliari University, Department of Mechanical, Chemical and Materials Engineering, via Marengo 2, 09123 Cagliari, Italy
[b] Imperial College London, Sargent Centre for Process Systems Engineering, Department of Chemical Engineering, SW7 2AZ London, UK

ARTICLE INFO

Editor: Prof. Rafiqul Gani

Keywords:
Power-to-liquid process
Direct air capture
Carbon dioxide
Global sensitivity analysis
Environmental analysis
Tecno-economic analysis

ABSTRACT

The power-to-liquid process is a key emerging technology for fossil-free raw materials and energy systems. In this work, techno-economic, and environmental analyses are carried out for a Fischer-Tropsch process producing diesel and characterized by the recovery of carbon dioxide through direct air capture, as well as the recovery of water and heat. The main aim of this study is to verify with respective analyses the circularity of carbon dioxide, water and heat and to conduct a global sensitivity analysis to identify significant system process parameters for some key performance indicators, when changed simultaneously. Despite the proven circularity based on material and energy balances ensuring a power-to-liquid efficiency of about 44 %, results show that the water closed loop is not ensured from an environmental point of view. The water consumption impact category is, in fact, a positive value (0.58–0.74 m^3depriv/kg_{diesel}), while the climate change impact category is a negative value (−1.22 to −0.28 $kgCO_{2eq}/kg_{diesel}$). A heat closed loop is attained according to the pinch analysis. The diesel production cost is competitive with the market price (1.76 and 2.07 $/$liter_{diesel}$ respectively when solar and wind energy are used). Regarding the sensitivity analysis, it is found that only costs and efficiency depend on the geographic location of the plant, in contrast to other key performance indicators. Overall, an additional optimization of the process is hence required to ensure a closed water loop from an environmental point of view and reduce further the production cost.

1. Introduction

After the COVID-19 pandemic, carbon dioxide (CO_2) emissions have been on the rise again, reaching 37.15 Gton (Giga metric tonne) in 2022 (OurWorldInData, 2023). The atmospheric CO_2 concentration is, consequently, expected to increase. Without efficient actions, it is projected that CO_2 levels could double by 2100 compared to the current level of 424 ppm, leading to a temperature increase of up to 6.1 °C compared to the 1990 level—a value much higher than the target (1.5 °C) set in the COP21 agreement (EIA, 2023). On the other hand, the Intergovernmental Panel on Climate Change (IPCC) report on the impacts of global warming estimates that that emissions must be limited to less than 420 $GtCO_2$/y to have a 67 % chance of limiting the global average temperature increase to 1.5 °C (IPCC, 2018).

For this reason, several strategies to reduce CO_2 emissions have been proposed, including reduction of energy and resource consumption, increasing the decarbonization rate and the utilization of carbon dioxide removal technologies (Marchese et al., 2021). In this context, the European Union has committed to achieve climate-neutrality by 2050 (European Commission, 2018). According to the previous strategies, this objective can be ensured by the utilization of non-fossil carbon sources (Buffo et al., 2020). In non-fossil applications, hydrogen can be obtained via water electrolysis by using renewable electricity (solar, wind and hydro energy etc.). In this way, the produced hydrogen can be combined with a renewable carbon feedstock, such as CO_2 captured with a particular technology, to produce syngas (a mixture of hydrogen, carbon monoxide and carbon dioxide). The obtained syngas is upgraded to synthetic fuels (e-fuels) (gasoline, kerosene, diesel, etc.) and chemicals (methanol, dimethyl ether, etc.). These products can be utilized within various industries or serve as raw materials for other compounds (Lehtonen et al., 2019; Dieterich et al., 2020; Rivera-Tinoco et al., 2016). This integrated system, known as power-to-liquid (PtL), is being discussed as a promising means to simultaneously reduce CO_2 emissions and provide compounds for a fossil-free society (Herz et al., 2021).

A power-to-liquid process typically includes a CO_2 capture technology, hydrogen production (usually from water electrolysis), and hydrocarbons synthesis via the Fischer-Tropsch (FT) route (Rojas-Michaga

* Corresponding author at: Cagliari University, Department of Mechanical, Chemical and Material Engineering, via Marengo 2, 09123 Cagliari, Italy.
E-mail address: grazia.leonzio@unica.it (G. Leonzio).

https://doi.org/10.1016/j.spc.2024.09.018
Received 4 August 2024; Received in revised form 18 September 2024; Accepted 24 September 2024
Available online 28 September 2024

Nomenclature

BAU	Business As Usual
CAPEX	Capital expenditures
CRF	Capital Recovery Factor
CEPCI	Chemical Engineering Plant Cost Index
DAC	Direct Air Capture
FT	Fischer-Tropsch
HC	Hydrocracking
IPCC	Intergovernmental Panel on Climate Change
KPI	Key Performance Indicator
LCA	Life Cycle Assessment
LCI	Life Cycle Inventory
LCIA	Life Cycle Impact Assessment
OPEX	Operating expenditures
PSA	Pressure Swing Adsorption
PtL	power-to-liquid
RWGS	Reverse Water Gas Shift

Symbols

η_{PtL}	power-to-liquid efficiency (%)
F_{diesel}	mass flow rate of produced diesel (kg/h)
LHV_{diesel}	low heating value of diesel (kWh/kg_{diesel})
$P_{electrolyser}$	electric power consumed by the electrolyser (kW)
$P_{utilities}$	electric power consumed by the utilities (kW)

et al., 2023). In particular, the fuel can be synthesized from CO_2 via an indirect route by combining the Reverse Water−Gas Shift (RWGS) reaction and the FT synthesis process, with syngas as an intermediate (Zang et al., 2021).

In the literature, several studies have investigated these particular systems, employing mathematical models of the process (Adelung et al., 2021; Marchese et al., 2020, 2021), conducting economic analysis to determine the levelized cost (Dieterich et al., 2020; Schmidt, 2016; Schmidt et al., 2018; Martín and Grossmann, 2011; Herz et al., 2021; Zhou et al., 2022) or performing environmental analyses to quantify impacts, such as climate change (Falter et al., 2016; Heidgen et al., 2019; Micheli et al., 2022; Yoo et al., 2022).

In several cases, diesel has been the main product investigated in these processes. For instance, Konig et al. (2015a) evaluated the carbon conversion (carbon in liquid fuels relative to carbon from CO_2) and power-to-liquid efficiency (energy in liquid fuels relative to electrical energy) of FT fuel derived from CO_2 and water, with electricity as the primary source of energy. Their simulation results indicated that the carbon conversion ratio is 73.7 %, and the power-to-liquid efficiency is 43.4 %.

Regarding the economic analysis of processes producing diesel, Peters et al. (2022) suggests a production cost between 1.02 and 2 $\$/liter_{diesel}$ when utilizing high temperature cell electrolysis, underlining the huge potential of the developed technology. On the other hand, the power-to-liquid efficiency ranges between 46 % and 67 % respectively for electrolyser efficiencies of 60 % and 100 %. A comparison between the current alkaline electrolyser and future solid oxide co-electrolysis using wind energy is reported in Heidgen et al. (2019)—with resulting e-fuel production costs respectively of 5.39 $\$/liter_{diesel}$ and 3.51 $\$/liter_{diesel}$ of diesel equivalent. It is evident that while e-fuels are currently not a cost-effective method to reduce CO_2 emissions they could be in the future if the investment cost, capacity utilization, CO_2 cost, and wind electricity cost can be improved by further research and development, or if fossil fuel prices increase substantially. The authors estimate in addition that life cycle emissions are currently 64.07 gCO_{2eq}/MJ_{diesel} while in the future they can be reduced to 6.63 gCO_{2eq}/MJ_{diesel}.

The environmental advantages of diesel production via a power-to-liquid process are reported in Samavati et al. (2018), where the system is able to reduce carbon emissions by 98–102 %. With an additional analysis, Isaacs et al. (2021) found that wind energy outperforms solar in carbon dioxide equivalent (CO_{2eq}) emissions, while a synergistic combination of both provides the best economic result. The advantages of using 100 % wind energy to produce hydrogen are also reported in Soler et al. (2022). In a cradle-to-gate system boundary the process located in the Central Europe and producing diesel emits 8.4 gCO_{2eq}/MJ_{diesel} if only wind energy is used compared to 13 gCO_{2eq}/MJ_{diesel} if a mix of solar and wind energy is used.

Carbon capture from ambient air is receiving significant attention lately. Research has been focusing on the carbon dioxide capture from the air through Direct Air Capture technologies that can be based on absorption, adsorption, membrane, cryogenic separation, etc. (Leonzio et al., 2022a, 2022b; Bisotti et al., 2024).

A few works have been presented in the literature about the integration of a Direct Air Capture (DAC) process into a Fischer Tropsch reactor with diesel as the main product. In Liu et al. (2020), the first LCA study of an absorption-based DAC integrated into a FT unit is carried out. Results show that 29 gCO_{2eq}/MJ_{fuel} are emitted considering a relatively low electricity emissions factor. It is found that an electricity emissions factor lower than 139 gCO_{2eq}/kWh is required to provide a climate benefit over conventional diesel fuel (104 gCO_{2eq}/MJ_{fuel}). A similar analysis is conducted by Medrano-García et al. (2022) where different renewable energy sources (wind, solar, nuclear, or the current mix) are compared for electricity production. The authors find that hydrogen from wind and nuclear energies could reduce the carbon footprint compared to fossil diesel, leading to burden-shifting in human health and ecosystems. However, a higher cost is obtained for the non-conventional production system. From an economic point of view, Fasihi et al. (2016) studied the synthesis of diesel from CO_2 captured from the air and a hybrid wind/solar electricity supply for alkaline electrolyzers for hydrogen production. Considering the O_2 valorization, they find that production costs can reach 0.75 $\$/liter_{diesel}$. An additional economic analysis is proposed by Soler et al. (2022), projecting that by 2050, the diesel production cost from a diluted source could reach a value of 2.08 $\$/liter_{diesel}$ equivalent for the Mediterranean Sea area, with electricity consumption having the highest impact on total cost.

All the above works show that linear processes have been mostly considered. However, through the integration of a DAC system into the fuel production process, it is possible to recover water and heat from the FT reactor to be used in the electrolysis and the direct air capture process, respectively. Moreover, the capture of carbon dioxide from the air allows simultaneous capture of atmospheric water. A similar integration for sustainable aviation fuel production is shown in Rojas-Michaga et al. (2023) and a higher energy efficiency should be ensured in this integrated solution compared to the conventional process. A question that arises from this consideration is if it is possible to produce fuels with a perfect circularity in carbon dioxide, water and heat. Mertens et al. (2023) report that a DAC system integrated into a fuel production process can potentially be self-sufficient in water and moreover, the heat produced in the process can supply the heat demand of the carbon dioxide capture technology. As the captured CO_2 is used for fuel production, a CO_2 closed loop is also ensured in addition to water and heat closed loops. However, a full life cycle assessment (LCA) is required to verify the sustainability of the process described and the proposed research tries to fill this gap.

In the literature, different mathematical models and software have been proposed for a sustainability analysis. The most common used model is life cycle assessment that can comprise three dimensions: environmental, social and economic. Common software tools based on this model are: SimaPro, Gabi, OpenLCA, Umberto and TESARREC (*TESARREC™ Trademark: UK00003321198*, 2018; Leonzio, 2024). The areas of research that have recently applied the LCA methodology include environmental engineering (Ahamed et al., 2020, 2021), energy (Stamford, 2020), chemical (Zhang et al., 2020; Dahiya et al., 2020), waste management (Berticelli et al., 2020), plastic recycling (Foolmaun and Ramjeawon, 2013), biomass strategies and biorefinery systems (Sadhukhan et al., 2019), building infrastructure (Llatas et al., 2020) and carbon supply chains (Leonzio et al., 2023a, 2023b).

According to these considerations, in this work, a mathematical model based on material and energy balances for a power-to-liquid process producing diesel, is developed. In the proposed system, a closed loop for CO_2, water and heat is considered as suggested in the literature while the main aim and novelty of this work is to quantify circularity and sustainability with a full life cycle assessment for the environmental dimension.

Based on the same mathematical model, a techno-economic analysis is also developed to evaluate the power-to-liquid efficiency and production cost. In addition, in this work, a Global Sensitivity Analysis (GSA) is carried out to identify the critical parameters that mostly influence techno-economic and environmental Key Performance Indicators (KPIs) (e.g. production cost, power-to-liquid efficiency, midpoint and endpoint impact categories, net amount of water produced inside the plant (Cucurachi et al., 2016; Groen et al., 2017)). It should be noted that global sensitivity analysis of a FT-based PtL process exists in the literature but is focusing on techno-economic aspects emphasising in this way the novelty of our research (Adelung, 2022).

2. Modelling

In the following section, a description of the investigated process with material and energy balances as well as, the description of the economic, environmental and uncertainty analyses are provided.

2.1. Process description

In the proposed process for producing e-diesel (in addition to gasoline and kerosene) from CO_2 and H_2, a DAC unit based on adsorption is integrated into the e-diesel synthesis section. This section comprises RWGS, Fischer-Tropsch (FT) and hydrocracking (HC) reactors, along with a distillation train and a boiler for tail gases. Additionally, electrolytic cells are utilized for hydrogen production. The plant is located in the US, in a hot and dry region (e.g. West Texas) (Sendi et al., 2022).

An internal closed loop for water, CO_2 and heat is ensured, as shown in Fig. 1: the captured CO_2 from DAC is sent to the RWGS reactor, while the water obtained as a by-product from the RWGS and FT reactors is sent to the electrolytic cell. Furthermore, the heat generated from the electrolyser, FT reactions and boiler is used for the regeneration stage of

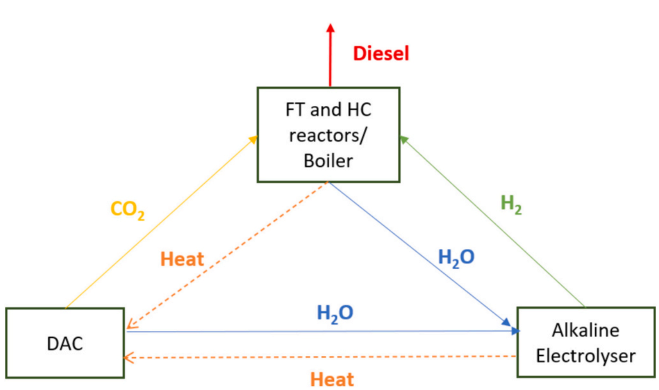

Fig. 1. Integration among processes of the whole plant (DAC = Direct Air Capture, FT = Fischer Tropsch, HC = Hydrocracking).

both DAC system and shift reaction. In Fig. 2 a complete scheme diagram of the investigated process is presented.

For each unit operation inside the considered process, the common assumptions reported in the literature and/or in a real operation plant are taken into account as reported below. The considered assumptions for a specific unit operation are related together: input and output of a specific process are connected together as reported in the literature from simulations works or as reported in real plants. For this reason, a mathematical model based on material and energy balances instead of a process simulation is proposed in this research (El-Halwagi, 2017).

The DAC system is based on adsorption according to the Climeworks plant in Switzerland (Hinwil) (Climeworks, 2020). The adsorption-based process is used as the simplest plant which is available at a commercial scale and which offers heat integration opportunities at the right temperature. Although the reported process considers 18 bed units, a single bed unit is taken into account in this work (area footprint excl. options of 20 m^2, length of 3.2 m with 135 kg/day of captured CO_2) as in Leonzio et al. (2022a, 2022b). The APDES-NFCFD (3-aminopropylmethyldiethoxysilane (APDES) on nanofibrillated cellulose (NFC)) is the sorbent used and temperature swing is the solution adopted for its regeneration so that the following stages occur: adsorption, desorption through temperature variation and cooling (Leonzio et al., 2022a, 2022b). In the process, the adsorption temperature is set as that of the air (25 °C), while the regeneration temperature is 100 °C because heat is supplied (Leonzio et al., 2022a, 2022b). Cooling water is used for the cooling step. The electricity for fans is provided by renewable electrical energy and heat for the desorption stage is provided by the heat released by the FT reaction and electrolyzers. The DAC unit captures CO_2 from the air with a temperature and relative humidity respectively of 25 °C and 39 % (CO_2 concentration is 400 ppm, neglecting the small amount of CO_2 that is recycled from C1–C4 combustion, having a flow rate of three order of magnitude lower compared to the amount of CO_2 captured from the air) (Sendi et al., 2022). The choice of an adsorption DAC process is critical in this analysis because requiring a lower amount of heat for the regeneration compared to a typical absorption process, it could help to achieve better the heat integration closed loop.

An alkaline cell, powered by wind renewable energy, is used to produce the hydrogen (H_2) needed for the RWGS synthesis. The cell works with an operating temperature and pressure of 50 °C and 24.5 bar respectively (Brauns and Turek, 2020; Sandeep et al., 2017). The inlet H_2/outlet H_2O mass ratio is fixed to 0.0664 (Soler et al., 2022), current density to 3000 A/m^2 (Hu et al., 2022), cell voltage to 1.8 V and Faradaic efficiency to 64 % (Sandeep et al., 2017). On the other hand, the voltage efficiency and electrical efficiency values are respectively 65 % (Soler et al., 2022) and 51.2 kWh/kg_{H2} (IRENA, 2020). During the electrolysis process, heat is released at a level of 14.65 kWh/kg_{H2} (Garcıa-Valverde et al., 2012). It is assumed that 90 % of water at the outlet is recycled into the feed while the other is sent to wastewater treatment.

In the RWGS reactor, the syngas required for the FT reaction is produced by using the CO_2 from DAC and H_2 from the electrolytic cell. The captured CO_2 is compressed from 1 bar to 24.5 bar before to be fed into the reactor. Operating temperature and pressure are respectively 600 °C and 24.5 bar (Zang et al., 2021; Kim et al., 2014). With an overall CO_2 conversion of 85 % and CO_2 conversion per pass of 36 % (Zang et al., 2021; Repasky and Zeller, 2021) the system is able to produce a syngas with H_2/CO ratio of 2.05, suitable for the FT synthesis (Konig et al., 2015b; Freire Ordonez et al., 2021). A CO_2 90 % of recycle ratio is set in order to reduce emissions and increase conversion (Freire Ordonez et al., 2021), while BaCe0.2Zr0.6Y0.16Zn0.04O3 is the used catalyst (Zang et al., 2021; Kim et al., 2014). As an endothermic reaction, the needed thermal energy is provided by the heat released by the FT reactor, alkaline cell and combustion of light gases in the boiler. The water obtained from the reaction synthesis is separated from the syngas through a flash and cooling system and sent to the electrolytic cell. CO_2

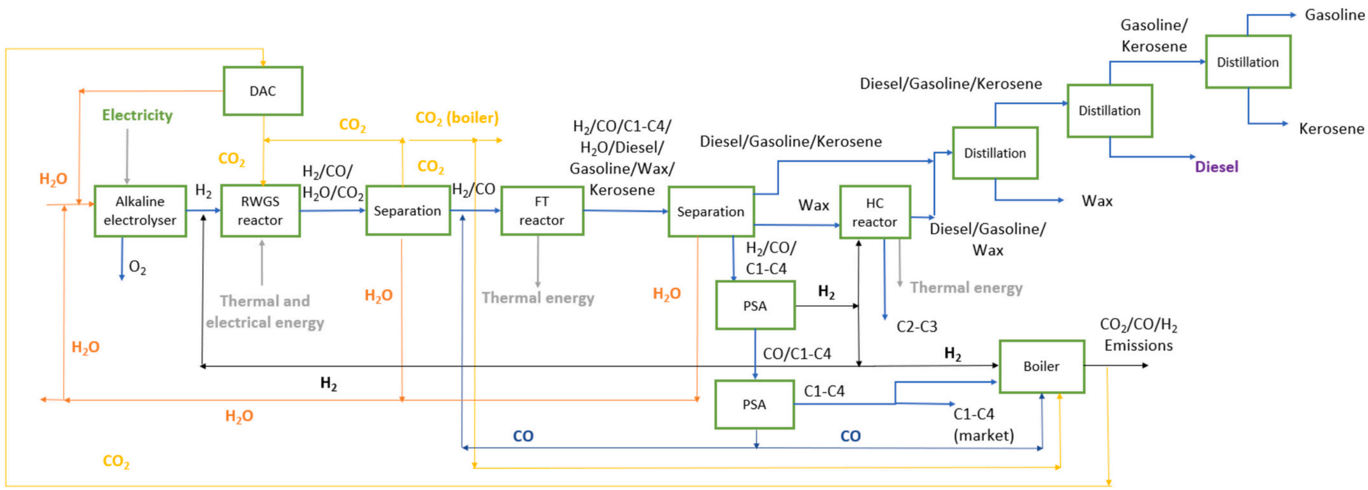

Fig. 2. Diagram scheme of the investigated diesel production process (DAC = Direct Air Capture, FT = Fischer Tropsch, HC = Hydrocracking, RWGS = Reverse Water Gas Shift, PSA = Pressure Swing Adsorption).

is recovered through the absorption technology (Zang et al., 2021).

The low temperature FT reactor catalytically converts the syngas into synthetic hydrocarbons by using a cobalt-based catalyst: polymerization reactions occur to transform CO and H_2 into liquid hydrocarbons or syncrude and into gaseous hydrocarbons, unreacted reactants and inert components (Zang et al., 2021; Hillestad, 2015; Freire Ordonez et al., 2021; Verdegaal et al., 2015). Operating temperature and pressure are respectively of 220 °C and 24.3 bar (Zang et al., 2021) while the overall and per-pass CO conversion are 80 % and 40 %, respectively (83 % of CO recycle ratio is fixed in order to increase the conversion reaction) (Konig et al., 2015b). At the outlet of FT reactor, we assume a product distribution as reported by Marion et al. (2006): C1 (8.32 *w*/w%) and C2–C4 (10.35 w/w%) as light hydrocarbons, C5–C9 (16.64 w/w%) as gasoline, C10–C13 (14.43 w/w%) as kerosene, C14–C21 (24.49 w/w%) as diesel, C22–C24 (4.78 w/w%) and C25+ (20.99 w/w%) as wax (e.g. a long paraffinic chain). From here the product flow rate is flashed so that, the wax is sent to the HC reactor and separated from the by-product water sent to the alkaline cell, gas products such as the C1–C4 mixture, CO and H_2 recovered through two Pressure Swing Adsorption (PSA) columns, and other liquid hydrocarbons. While CO is recycled to the reactor feed, the recovered H_2 is both recycled to the RWGS reactor (the recycle ration is fixed at 68 % in order to have enough H_2 in the hydrocracking reactor) and sent, in the remaining part, to the HC section (Zang et al., 2021). The C1–C4 mixture can be sold like a gas product (HPV, 2009) and in part burnt into the boiler to supply the heat required to close the heat loop. The CO_2 emitted from the combustion is recycled to the DAC system. Other liquid hydrocarbons, mixed with the liquid flow rate coming from the HC reactor, are sent to a separation train of three distillation columns (Medrano-García et al., 2022). Regarding the heat released during the FT reaction, the overall reaction enthalpy variation is 37.4 $kcal/mol_{CO}$ (with a reaction rate of $5.34 \bullet 10^{-5}$ $mol/s/g_{cat}$) (Fratalocchi et al., 2018).

The wax from the FT synthesis is sent to the hydrocracking reactor with the recovered H_2 (H_2/wax mass ratio of 0.11 (Kang et al., 2012)), breaking the long hydrocarbon chain. Wax is cracked with a conversion of 84 % at 290 °C and 23.2 bar, over a Pt/Si-Al catalyst, ensuring the following product distribution: C12-C19 (52.4 w/w %) as diesel, C2-C3 (0.03 w/w %) as light hydrocarbons, C4–C11 (33.5 w/w%) as gasoline and kerosene mixture, wax (14.1 w/w%) (Kang et al., 2012; Freire Ordonez et al., 2022). The Pt-based catalyst is selected because it has a high hydrogenation/dehydrogenation activity for heavy hydrocarbon cracking and the produced wax is a sulphur free product (Lee et al., 2010; Calemma et al., 2010). For the wax the heating value is 41 MJ/kg_{wax} (Kang et al., 2012) while light gas hydrocarbons are sold.

The desired product (e.g. e-diesel) is produced via distillation. In the first distillation column of the separation train, the hydrocarbon feed is separated into wax and mixture of diesel, gasoline and kerosene while, in the second distillation column, the diesel is recovered from the feed mixture. In the last distillation column, kerosene and gasoline are obtained (Medrano-García et al., 2022). It is assumed that the overall heat and cooling requirement for the distillation train is respectively of 0.58 kWh/kg_{diesel} and 0.9 kWh/kg_{diesel} (Medrano-García et al., 2022).

All gas combustible residues (CO and H_2) are combusted with air in a boiler at 1000 °C and ambient pressure to generate heat supplied to the integrated process (Zang et al., 2021). For the combustion reaction, conversions are set to 90 % with an air excess of 20 %.

2.2. Mathematical model and pinch analysis

For the analysis of the proposed scheme, a mathematical model based on material and energy balances is developed. All considered equations are reported in the supplementary information (section S1, Tables S1–S4) and these are used for the economic, environmental and global sensitivity analyses. Through the mathematical model it is possible to evaluate in addition to the cost and environmental impact the overall power-to-liquid efficiency (η_{PtL}) and net water consumption of the integrated process, defined by the following equations (see Eqs. (1)–(2)) (Konig et al., 2015b):

$$\eta_{PtL} = \frac{F_{diesel} \bullet LHV_{diesel}}{P_{electrolyser} + P_{utilities}} \tag{1}$$

$$\begin{aligned} \text{Net water consumption} = & \text{ Water needed by electrolyser} \\ & - \text{Water produced by DAC} \\ & - \text{Water produced by reactions (FT + RWGS)} \end{aligned} \tag{2}$$

With F_{diesel} being the mass flow rate of produced diesel (kg/h), LHV_{diesel} the low heating value of diesel (11.8 kWh/kg_{diesel}), $P_{electrolyser}$ the electric power consumed by the electrolyser (kW), $P_{utilities}$ the electric power consumed by CO_2 compressors (kW), cooling water (DAC and distillation columns) (kW) and funs for DAC (kW) (as reported in the supplementary information), Net water consumption the overall water consumption in the plant (kg/h), Net heat consumption the overall heat consumption in the plant (kW), water needed by electrolyser the water required for the alkaline cell (kg/h), water produced by DAC the water obtained from CO_2 capture (kg/h), water produced by reactions (FT + RWGS) the water produced by FT and RWGS reactions (kg/h).

For the evaluation of the heat closed loop, a pinch analysis is conducted due to the different temperature levels of heat. The analysis is used to construct the table cascade finding the additional amount of C1–C4 flow rate to be combusted in order to have an autothermal process (e.g. heat closed loop) (Smith, 2005).

2.3. Economic analysis

Based on material and energy balances, capital (CAPEX) and operating (OPEX) expenditures are evaluated for the investigated process in order to find the total levelized production cost of diesel. For the evaluation of this production cost the following correlations are used (See Eqs. (3)–(6)), assuming an interest rate of 10 %, an economic plant lifetime of 20 years, an utilization of 91.3 %, an annual production in ton per year and an allocation factor by energy content among all liquid and gas products, for diesel of 37 % (Leonzio et al., 2023a, 2023b). In those correlations, the CAPEX is in \$, OPEX in \$/year, levelized CAPEX, OPEX and total levelized production cost are in \$/liter$_{diesel}$.

$$\text{Levelized CAPEX} = \frac{\text{CAPEX} \bullet \text{CRF}}{\text{Annual production} \bullet \text{Utilization}} \tag{3}$$

$$\text{CRF} = \frac{\text{interest rate} \bullet (1 + \text{interest rate})^{\text{plant lifetime}}}{(1 + \text{interest rate})^{\text{plant lifetime}} - 1} \tag{4}$$

$$\text{Levelized OPEX} = \frac{\text{OPEX}}{\text{Annual production} \bullet \text{Utilization}} \tag{5}$$

$$\text{Total Levelized Production Cost} = \text{Levelized CAPEX} + \text{Levelized OPEX} \tag{6}$$

The CAPEX is evaluated according to Becker et al. (2012), from the equipment expenditures by evaluating direct and indirect capital expenditures as well as contingencies and working capital. In particular, equipment expenditures are obtained for the main items: adsorbent bed, alkaline electrolyser, FT, RWGS and HC reactors, compressors, three distillation columns (for diesel, kerosene and gasoline separation), two PSA columns (for H_2, CO and C1–C4 separation) and boiler. A 12 % factor is added to total equipment expenditure to find the total direct expenditure while indirect expenditures are estimated to be 51 % of the direct capital expenditures (Becker et al., 2012; Spath et al., 2005). The total capital investment is then provided by summing direct and indirect capital expenditures (fixed capital investment) with contingencies and working capital (1.25 time the fixed capital investment) (Konig et al., 2015b).

For the equipment expenditure it is assumed that the DAC and electrolyser costs respectively 644 \$year/tonCO_2 (Leonzio et al., 2022a, 2022b) and 665 \$/kW (Bertuccioli et al., 2014), while for other items the expenditure is evaluated by the following equation (Konig et al., 2015b) (See Eq. (7)):

$$\text{Cost} = \text{Cost}_{ref} \bullet \left(\frac{S}{S_{ref}}\right)^{n} \bullet \left(\frac{\text{CEPCI}_{2023}}{\text{CEPCI}_{ref}}\right) \tag{7}$$

enabling estimation of the purchased cost of equipment at the scale (S), based on the reference cost (Cost$_{ref}$) at the reference scale (Sref) and considering an appropriate Chemical Engineering Plant Cost Index (CEPCI) for the reference year (402 for 2003, 576.1 for 2014, 521.9 for 2009) and a CEPCI value of 802.6 for 2023 (Toweringskills, 2024). The scaling factor (n) accounts for scaling effects. Table 1 shows all these data for FT, RWGS and HC reactors, distillation column, boiler, CO_2 compressors and PSA.

The OPEX is composed of maintenance, insurance, taxes, raw materials and utilities (Konig et al., 2015b). The maintenance expenditure for the electrolytic cell is evaluated as 15 % of the fixed capital investment while for the rest of the plant it is assumed as 7 % of the fixed capital investment (Konig et al., 2015b). Insurance and taxes are 2 % of the overall fixed capital investment while the expenditure for sorbent is 1.16 \$/kg, for cooling water it is 0.06 \$/m^3, for process water it is 0.41 \$/m^3 (Intratec, 2024) and for electricity from solar and wind energy it is respectively 0.06 \$/kWh and 0.03 \$/kWh (OurWorldInData, 2024).

2.4. Environmental analysis

The environmental impact of the integrated processes producing diesel is carried out according to the principles of Life Cycle Assessment (LCA) with the following standard phases as suggested by the ISO 14040: goal and scope definition, life cycle inventory (LCI), life cycle impact assessment (LCIA) and interpretation (ISO 14040, 2009; ISO 14044, 2006).

In the goal and scope definition, the aim of the analysis is defined as the evaluation of the environmental burden of the investigated production process to assess water and carbon dioxide closed loops and for a comparison with the conventional route (e.g. Diesel from refinery in the Ecoinvent database). For this purpose, the LCA is carried out considering 1 kg of diesel as the functional unit (the reference to which all inputs and outputs of the specific process are related) and cradle-to-gate system boundaries (the use of diesel is outside the evaluation of the environmental burden because only processes from raw material extraction up to diesel production are analyzed). An allocation by mass is assumed in processes where more products are present.

In the second phase of LCA, inventory data (e.g. material and energy balances of the considered processes) are evaluated and obtained from the modelling study as described in Section 2.1, because they are unavailable in the Ecoinvent database so that they are considered as new processes in the OpenLCA software. The inventory data for all investigated processes are reported in the Tables 2 and 3.

In Table 2, the inventory data for the whole electrolytic cell, reactors, boiler and distillation section integrated into the DAC system is shown. The heat in the output stands for the net overall heat of the process. On the other hand, the water in the input stands for the net overall water of the process. In Table 3, the inventory data for the DAC plant are reported: the needed thermal energy is not present among inputs because heat is supplied by the process while water is not present as product in the output because it is used by the electrolytic cell.

In the following phase of LCA, i.e. LCIA, the LCI results are generated and organized into the impact category and then into the impact indicator at the midpoint level (climate change and water use) and endpoint level (human health, ecosystem quality, resources). The ReCiPe 2016 method is used to evaluate the climate change and endpoint impact

Table 1
Cost parameters for the economic analysis of the integrated process (FT = Fischer Tropsch, RWGS = Reverse Water Gas Shift, HC = Hydrocracking, PSA = Pressure Swing Adsorption).

	Reference cost		Reference size		Scaling factor	Reference time	Reference
FT reactor	10.5	M\$	2.52	Mscf/h (Feed flow rate)	0.72	2003	Freire Ordonez et al. (2021)
RWGS reactor	2.6	M\$	2556	ton/day (Feed flow rate)	0.65	2014	Freire Ordonez et al. (2021)
HC reactor	8.46	M\$	1.13	kg/s (Feed flow rate)	0.7	2014	Freire Ordonez et al. (2021)
Distillation	0.73	M\$	6.59	ton/h (Feed flow rate)	0.7	2009	Marchese et al. (2021)
Boiler	2.14	M\$	20	MW (Duty)	0.8	2014	Freire Ordonez et al. (2021)
PSA	5.46	M\$	0.294	kmol/s (Purge gas flow)	0.74	2003	Becker et al. (2012)
CO_2 compressor	4.75	M\$	10	MWe (Compression power)	0.67	2003	Larson et al. (2005)

Table 2
Inventory data for system composed by the alkaline electrolyser, FT, RWGS and HC reactors, boiler and distillation columns and integrated into the DAC system (at air temperature and humidity of 25 °C and 39 %) (FT = Fischer Tropsch, RWGS = Reverse Water Gas Shift, HC = Hydrocracking).

Inputs		
H_2O	0	kg/kg_{diesel}
CO_2	2.75	kg/kg_{diesel}
Electricity for water electrolysis	0.03	MWh/kg_{diesel}
Electricity for CO_2 compressor	0.0002	MWh/kg_{diesel}
Air for boiler	0.78	kg/kg_{diesel}
Cooling water, make up (distillation train)	0.001	kg/kg_{diesel}
Electricity for cooling water (distillation train)	0.03	kWh/kg_{diesel}
Outputs		
O_2	1.32	kg/kg_{diesel}
H_2 emissions	0.0002	kg/kg_{diesel}
CO emissions	0.02	kg/kg_{diesel}
H_2O from electrolyser	0.01	kg/kg_{diesel}
Heat	0.008	MWh/kg_{diesel}
C_2–C_3 from HC to market	0.0002	kg/kg_{diesel}
Gasoline from FT	0.79	kg/kg_{diesel}
Kerosene from FT	0.37	kg/kg_{diesel}
Gasoline-Kerosene mixture from HC	0.24	kg/kg_{diesel}
C_1–C_4 from FT to market	0.41	kg/kg_{diesel}
Wax from HC	0.10	kg/kg_{diesel}
Diesel from FT and HC	1	kg

Table 3
Inventory data for the DAC system integrated into the whole process (at air temperature and humidity of 25 °C and 39 %).

Input		
Adsorption step		
Mass sorbent	2.88	$kg/tonCO_2$
Electricity for fans	224.84	$kWh/tonCO_2$
Air	63,316,676	$mol/tonCO_2$
CO_2	1101	$kg/tonCO_2$
N_2	1,367,243	$kg/tonCO_2$
O_2	419,027	$kg/tonCO_2$
Ar	23,368	$kg/tonCO_2$
H_2O	14,153	$kg/tonCO_2$
Cooling step		
Cooling water, make up	2178	$kg/tonCO_2$
Electricity cooling water	51.6	$kWh/tonCO_2$
Output		
Technosphere		
CO_2	1	ton
Emissions to air		
CO_2	101	$kg/tonCO_2$
N_2	1,367,243	$kg/tonCO_2$
O_2	419,027	$kg/tonCO_2$
Ar	23,368	$kg/tonCO_2$
H_2O	13,600	$kg/tonCO_2$

categories while the Environmental Footprint method is used to measure the water use impact category, by using OpenLCA software (version 1.11) and the Ecoinvent database 3.9. In this analysis, water use is considered instead of water consumption because the former establishes the total water use while the latter includes water that is lost to the ecosystem and for downstream users (Sphera, 2022).

In the last stage of LCA, i.e. the interpretation, results obtained in the previous phase are discussed and compared with the literature.

2.5. Uncertainty and global sensitivity analysis

An uncertainty analysis and a global sensitivity analysis (GSA) are conducted for several process key performance indicators (KPIs). Firstly, the uncertainty analysis is performed to quantify the variability of the KPIs, indicating how uncertain they are if specific uncertain operational parameters are varied simultaneously (Saltelli et al., 2010). Then GSA is used to find which uncertainty parameters are significant for the selected KPIs through the evaluation of Sobol sensitivity indices. The uncertain parameters and suitable ranges are identified from the literature. The uncertain parameters considered are air temperature, air humidity, amount of captured CO2, voltage efficiency, electrical efficiency, current density, cell pressure, cell temperature, CO_2 recycle ratio, and CO recycle ratio. The monitored KPIs are the PtL efficiency, production cost, net amount of water inside the plant, as well as the midpoint and endpoint impact categories.

A set of 1408 quasi-random input scenarios is generated based on the parameter ranges outlined in Table S5 of the supplementary information (Section 11.8), assuming a triangular distribution. The Sobol quasi-random sequence is employed as the sampling technique to ensure thorough exploration of the model input space. The input samples are then used to evaluate the desired KPIs by using the reported mathematical model for techno-economic KPIs and OpenLCA linked to Python for the environmental KPIs. Subsequently, GSA is conducted using the SobolGSA software (Kucherenko, 2013). Total-order Sobol sensitivity indices are computed to determine whether the uncertainty parameter is significant for the KPIs (Kucherenko and Song, 2017; Sobol, 2001). In this study, we utilize the Random Sampling-High Dimensional Model Representation (RS-HDMR) surrogate modelling method for the evaluation of Sobol indices.

3. Results and discussion

In this section, results for both the nominal case study, as well as the uncertainty and global sensitivity analysis regarding power to liquid efficiency, costs and environmental burden are reported. The results of mass and energy balances of the proposed mathematical model are shown.

3.1. Results of the nominal case study

3.1.1. Results for the process modelling

Based on material and energy balances described in the Supplementary Information (section S1), the integrated pilot-scale process located in a hot and dry region of the US (at an air temperature and humidity respectively of 25 °C and 39 %) can produce 18 ton/year (2 kg/h) of diesel with the overall amount of CO_2 captured from the air (135 kg/day). As all captured CO_2 is used to produce the fuel, a CO_2 closed loop is ensured. The net water consumption is 0 kg while an additional amount of heat (2.34 kW, obtained by sending a fraction of C1–C4 gases, as the 14 % of total molar flow rate, to the boiler) is required to satisfy a closed heat loop as found through the pinch analysis (a table cascade is reported in Section 2 of the Supplementary Information, particularly Table S8, in addition to Tables S6 and S7 according to Fig. S1) (Smith, 2005). It is verified that, based on material balance, the proposed integrated process is able to ensure a circularity for water, CO_2 and heat for the defined values of air temperature and humidity as also suggested by Mertens et al. (2023). The DAC-e-fuel process is self-sufficient in water and heat (the slightly upgrading of heat from the electrolysis at 50 °C to higher temperatures is required and might be obtained by mixing with higher temperature waste heat from the synthesis process) (Mertens et al., 2023).

Mass consumption and production of the process are reported in Table 4. Capturing 5.63 kg/h of CO_2, the system is able to produce 2 kg/

Table 4
Main results for the material balance of the integrated process producing 2 kg/h of diesel (RWGS = Reverse Water Gas Shift, DAC = Direct Air Capture, FT = Fischer Tropsch, HC = Hydrocracking).

Captured CO_2 for RWGS	5.63	kg/h
Air for boiler	4.95	kg/h
H_2O produced by DAC	3.09	kg/h
H_2 produced by electrolyser	0.66	kg/h
O_2 produced by electrolysis	2.67	kg/h
H_2O produced by FT and HC	3.3	kg/h
H_2O by-product from electrolysis	0.02	kg/h
H_2 emissions (boiler)	0.0005	kg/h
CO emissions (boiler)	0.05	kg/h
C1–C4 (boiler and market)	0.96	kg/h
C2–C3 (market)	0.0004	kg/h
Gasoline	1.35	kg/h
Kerosene	0.74	kg/h
Wax	0.21	kg/h
Total diesel	2.00	kg/h

h of diesel, 1.35 kg/h of gasoline, 0.74 kg/h of kerosene and 0.21 kg/h of wax, in addition to gas hydrocarbons that can be sold into the market (0.96 kg/h of C1-C4 and 0.0004 kg/h of C2–C3). At 298 K and 39 % of relative humidity, the DAC process can produce 3.09 kg/h of water, sent to the alkaline electrolyser with the other water from FT and RWGS reactions (3.3 kg/h). Emissions are coming from the boiler and RWGS reactor in the following amount: 0.046 kg/h of CO and 0.0005 kg/h of H_2. The alkaline electrolysis, in addition to the H_2, can produce both 2.67 kg/h of O_2 (that can be sold into the market) and the not internal recycled water sent to a wastewater treatment (0.022 kg/h).

Table 5 shows the energy consumption of the investigated process. Among electrical energy needs, the alkaline electrolyser has the highest impact (53 kW as 96 % of the overall requirement) while the lowest contribution is due to the cooling of the plant (0.05 kW as 0.18 % of the overall need). The highest impact of electricity for the electrolytic cell is also reported in Marchese et al. (2021). Regarding the thermal energy, DAC is the most endothermic system requiring 8.3 kW of heat while the HC reactor is the most exothermic process producing 11 kW of heat.

The overall power-to-liquid efficiency is 43.5 % in agreement with other results reported in the literature by Marchese et al. (2021) where this efficiency has a range between 28.06 % and 52.2 %. In that evaluation, the electrical power required for the electrolytic cell has the greatest influence, amounting to about 95 % of total electricity input (Peters et al., 2022).

Table 5
Main results for the energy balance of the integrated process producing 2 kg/h of diesel (RWGS = Reverse Water Gas Shift, DAC = Direct Air Capture, FT = Fischer-Tropsch, HC = Hydrocracking).

Electrical energy for funs in DAC	1.2	kW	
Electrical energy for cooling water in DAC	0.29	kW	
Electrical energy for alkaline electrolyser	53	kW	
Electrical energy for CO_2 compressors	0.5	kW	
Electrical energy for cooling in the distillation train	0.065	kW	(Medrano-García et al., 2022)
Thermal energy for DAC	8.3	kW	
Thermal energy for RWGS	1.85	kW	
Thermal energy for distillation train	1.17	kW	(Medrano-García et al., 2022)
Thermal energy from FT reactor	3.28	kW	
Thermal energy from HC reactor	11	kW	
Thermal energy from alkaline electrolyser	6.6	kW	
Thermal energy from boiler (CO and H_2 combustion)	0.005	kW	
Thermal energy from boiler (C1–C4 combustion)	2.35	kW	

3.1.2. Results for the economic analysis

Results of the economic analysis for the plant located in the US with an air temperature and humidity of 25° and 39 % are shown in Table 6. With an overall CAPEX of 42,400 \$/year and OPEX of 38,300 \$/year the total levelized production cost of diesel is 1.76 \$/liter$_{diesel}$ (49 \$/GJ$_{diesel}$), when wind energy is used for the renewable electricity. When solar energy is used to produce renewable electricity, OPEX are 53,305 \$/year and the production cost is 2.07 \$/liter$_{diesel}$ (58 \$/GJ$_{diesel}$).

The value for diesel production cost from CO_2 is in line with the literature even though a slight lower cost can be obtained due to circularity that allows cost savings for some thermal energy and water consumption (Soler et al., 2022; Peters et al., 2022; Schemme et al., 2017). In fact, production cost up to 4.29 \$/liter$_{diesel}$ are reported in the existing literature (Soler et al., 2022). Diesel production cost of the proposed scheme with circularity in water, CO_2 and heat is also competitive with the market price in the US equal to 1.022 \$/liter$_{diesel}$ (GlobalPetrolPrices, 2024). The proposed integrated scheme at the defined air temperature and humidity enables a diesel production cost that is lower compared to the values reported in the literature and competitive with the conventional production showing in this way economic advantages in comparison with the linear process not exploiting renewable energies and capturing CO_2 from the air. A further cost reduction could be ensured through the use of carbon credits, that, like economic incentives, could make the process more convenient compared to the market.

Table S9 of the supplementary information (Section 3) shows a detailed analysis of equipment cost. Among the total installed cost, the FT and HC reactors have the highest impact, respectively contributing 23 % and 25 %. On the other hand, the distillation column for kerosene separation has the lowest impact on total equipment costs (0.36 %). The electrolytic cell system has an impact on equipment cost of about 9 %, as similarly obtained by Becker et al. (2012) while DAC contributes 17 % of the total equipment cost, in line with the figures reported by Marchese et al. (2021) even though an absorption system is used in their work. However, a detailed comparison with previous research is difficult because most of the work uses CO_2 capture cost as input for their economic assessment (Rojas-Michaga et al., 2023).

It is important to underline that the electricity cost for water electrolysis has the greatest influence on total cost of raw materials and utilities (95 % for wind-based electricity). The importance of the electrolytic cell on cost is well reported in the literature (Konig et al., 2015b; Dieterich et al., 2020; Medrano-García et al., 2022). On the other hand, the cost for the all-electricity consumption is 38 % of the overall OPEX while the maintenance cost of plant and electrolyser and insurance and taxes are respectively 28 %, 13 % and 18 % of the whole OPEX (when electricity from wind is used).

Overall, due to the low electricity price, CAPEX expenditures have a higher impact on total costs when electricity from wind is used: they are 55 % of the levelised production cost. This means that to minimize total costs, the optimal design of equipment is required in addition to the

Table 6
Results of the economic analysis for the integrated process at different electricity energy sources.

	Wind energy	Solar energy	
Total installed cost	182,259	182,259	\$
Total direct cost	204,130	204,130	\$
Total indirect cost	104,106	104,106	\$
Fixed capital investment	308,237	308,237	\$
Capex	42,383	42,383	\$/year
Maintenance cost of the plant	11,056	11,056	\$/year
Maintenance cost of the electrolyser	2599	2599	\$/year
Insurance and taxes	6165	6165	\$/year
Utilities and raw materials	15,182	30,193	\$/year
Opex	38,294	53,305	\$/year
Total levelized diesel production cost	1.76	2.07	\$/liter$_{diesel}$

increase of plant scale. The opposite situation occurs when electricity from solar energy is used: CAPEX expenditures are 47 % of the total cost. The same situation is obtained when electricity from the grid is used (at an electricity cost of 0.15 $/kWh (GlobalPetrolPrices, 2024)): OPEX expenditures are 67 % of the total expenditures and a diesel production cost is 2.98 $/liter$_{diesel}$. In this case, the PtL process is OPEX dependent (Rojas-Michaga et al., 2023).

3.1.3. Results for the environmental analysis

Midpoint (climate change and water use) and endpoint (human health, ecosystem quality and resources) impact categories are evaluated for the integrated process analyzed in this work considering wind and solar energy for the electricity production and are compared with the conventional process producing diesel as reported in the Ecoinvent database. The results are provided for an air temperature and humidity of 25 °C and 39 %, respectively, according to a cradle-to-gate analysis. In particular, Fig. 3 shows the results for the midpoint impact categories, climate change and water use, for 1 kg of diesel production: the proposed scheme allows to have an environmental impact lower compared to that of the business as usual (BAU) process (e.g. diesel from refinery reported in the Ecoinvent database).

Values of climate change for the proposed scheme exploiting wind and solar energy are respectively −1.22 $kgCO_{2eq}/kg_{diesel}$ and −0.28 $kgCO_{2eq}/kg_{diesel}$ while the conventional process emits 0.58 $kgCO_{2eq}/kg_{diesel}$. It is evident that the power-to-liquid process has the potential to decrease greenhouse gas emissions and decarbonize the energy sector. Negative values of climate change are obtained meaning that a mitigation of CO_2 emissions is achieved as cradle-to-gate system boundaries are considered.

On the other hand, the water circularity ensures for the investigated process values of water use lower compared to that of the conventional process (0.74 $m^3depriv/kg_{diesel}$ and 0.58 $m^3depriv/kg_{diesel}$ when solar and wind energy are respectively used vs 14.1 $m^3depriv/kg_{diesel}$ for the BAU system). The trends are similar to those found in the Medrano-García et al. (2022), i.e., wind energy performs better than solar energy in fuel production.

A negative value of climate change is not suggesting the CO_2 removal from the atmosphere because a cradle-to-gate analysis is considered here. However, a mitigation of CO_2 and a CO_2 closed loop are obtained. Then, for the proposed scheme, the CO_2 closed loop is verified from a mathematical and environmental analysis point of view. Concerning the impact breakdown when solar and wind energy are used, the highest contribution with a positive effect on climate change is the electricity consumption (1.33 $kgCO_{2eq}/kg_{diesel}$ for solar energy and 0.42 $kgCO_{2eq}/kg_{diesel}$ for wind energy), while CO_2 capture is the highest negative impact on climate change (−2.47 $kgCO_{2eq}/kg_{diesel}$ in both case studies). An improvement of the energy efficiency of the system and reduction of the carbon footprint of the electricity source (by improving construction, maintenance, and operation stages) are suggested (Rojas-Michaga et al., 2023).

Regarding the water use, the proposed scheme has a value close to 0 in both case studies (when wind and solar energies used for electricity production) against the results obtained from the mathematical model. The full LCA suggests that an additional optimization of the process is required in order to have a water closed loop also from an environmental analysis point of view. When solar energy is used, electricity production through collectors and cooling water have the highest impact on total water use value respectively of 51 % and 49 %. An electricity source that is more environmentally friendly for water use and a reduction of cooling water are required. In this context, the optimization of energy and cooling water systems has been also suggested in the literature by Rojas-Michaga et al. (2023) to reduce the water footprint of a sustainable aviation fuel production process.

Overall, a direct comparison with the literature cannot be conducted because only absorption-based DAC systems are used in previous works regarding diesel production from CO_2 (Medrano-García et al., 2022; Liu et al., 2020). However, for works investigated in the literature good values of climate change potential are reported for diesel production, as found in this proposed research (Rojas-Michaga et al., 2023). Only water consumption is shown in the literature hence a direct comparison with the investigated work cannot be done for the water use impact category.

Results for other mid-point impact categories, according to the ReCiPe 2016 method, are reported in Table 7: even though climate change and water use are better for the integrated process compared to the conventional one, the suggested system has a worse environmental burden in freshwater ecotoxicity, freshwater eutrophication, human carcinogenic toxicity, human non-carcinogenic toxicity, land use, marine ecotoxicity, marine eutrophication, mineral resource scarcity and terrestrial ecotoxicity when wind energy is used for electricity production. On the other hand, when solar energy is used the following impact categories are worse compared to the BAU process: fine particulate matter formation, freshwater ecotoxicity, freshwater eutrophication,

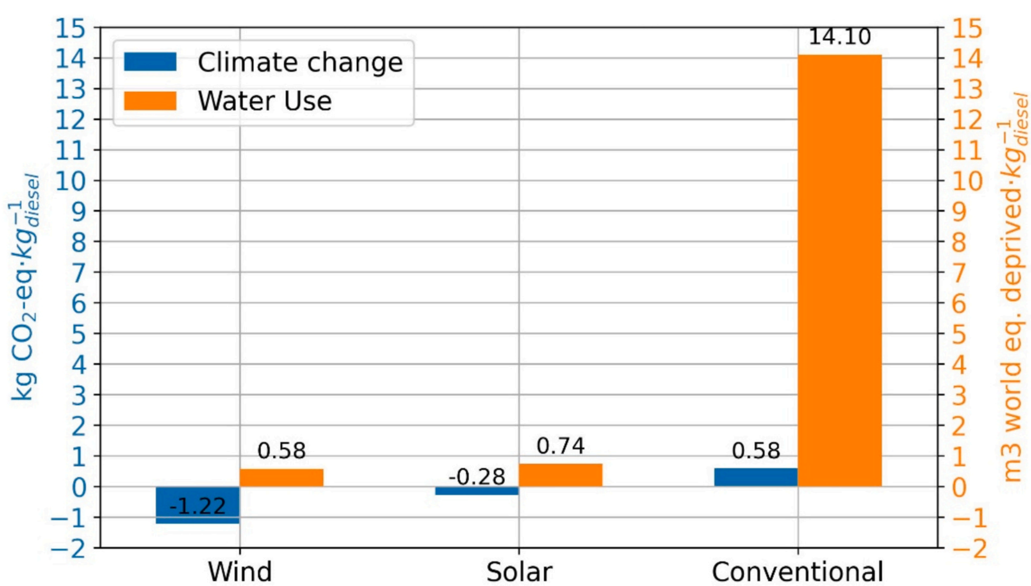

Fig. 3. Results of the midpoint impact categories for the integrated process at the nominal case study and a comparison with the BAU.

Table 7
Results for the mid-point impact categories (ReCiPe 2016 method).

Impact category	Reference unit	Electricity from wind energy	Electricity from solar energy	Conventional process
Fine particulate matter formation	kg $PM_{2.5eq}/kg_{diesel}$	0.0009	0.0020	0.0015
Fossil resource scarcity	kg oil_{eq}/kg_{diesel}	0.12	0.47	1.22
Freshwater ecotoxicity	kg 1,4-DCB/kg_{diesel}	0.20	0.10	0.007
Freshwater eutrophication	kg P_{eq}/kg_{diesel}	0.0002	0.0003	3.45E-05
Human carcinogenic toxicity	kg 1,4-DCB/kg_{diesel}	0.12	0.10	0.009
Human non-carcinogenic toxicity	kg 1,4-DCB/kg_{diesel}	1.30	1.12	0.19
Ionizing radiation	kBq Co-$60_{eq}/kg_{diesel}$	0.021	0.027	0.0333
Land use	m2a $crop_{eq}/kg_{diesel}$	0.16	0.32	0.027
Marine ecotoxicity	kg 1,4-DCB/kg_{diesel}	0.25	0.14	0.01
Marine eutrophication	kg N_{eq}/kg_{diesel}	$2.95 \bullet 10^{-5}$	$5.9 \bullet 10^{-5}$	$4.47 \bullet 10^{-6}$
Mineral resource scarcity	kg Cu_{eq}/kg_{diesel}	0.014	0.038	0.0009
Ozone formation, Human health	kg NOx_{eq}/kg_{diesel}	0.001	0.004	0.002
Ozone formation, Terrestrial ecosystems	kg NOx_{eq}/kg_{diesel}	0.001	0.004	0.002
Stratospheric ozone depletion	kg $CFC11_{eq}/kg_{diesel}$	$2.51 \bullet 10^{-7}$	$1.13 \bullet 10^{-6}$	$9.76 \bullet 10^{-7}$
Terrestrial acidification	kg $SO2_{eq}/kg_{diesel}$	0.0017	0.0045	0.0046
Terrestrial ecotoxicity	kg 1,4-DCB/kg_{diesel}	5.49	3.93	1.90

human carcinogenic toxicity, human non-carcinogenic toxicity, land use, marine ecotoxicity, marine eutrophication, mineral resource scarcity, ozone formation (human health), ozone formation (terrestrial ecosystems), stratospheric ozone depletion. These results suggest that a better trade off must be achieved in the innovative process with the aim to be more environmentally friendly compared the BAU in all impact categories.

Fig. 4 shows results for the endpoint impact categories: human health in Fig. 4a, resources in Fig. 4b and ecosystem quality in Fig. 4c. In all impact categories the conventional process has an environmental burden higher compared to the process based on water, heat and CO_2 circularity. Human health values for the BAU system, integrated process using solar and wind energy are respectively of $1.87 \bullet 10^{-6}$ DALY/kg_{diesel}, $1.60 \bullet 10^{-6}$ DALY/kg_{diesel} and $4.03 \bullet 10^{-7}$ DALY/kg_{diesel}. In both

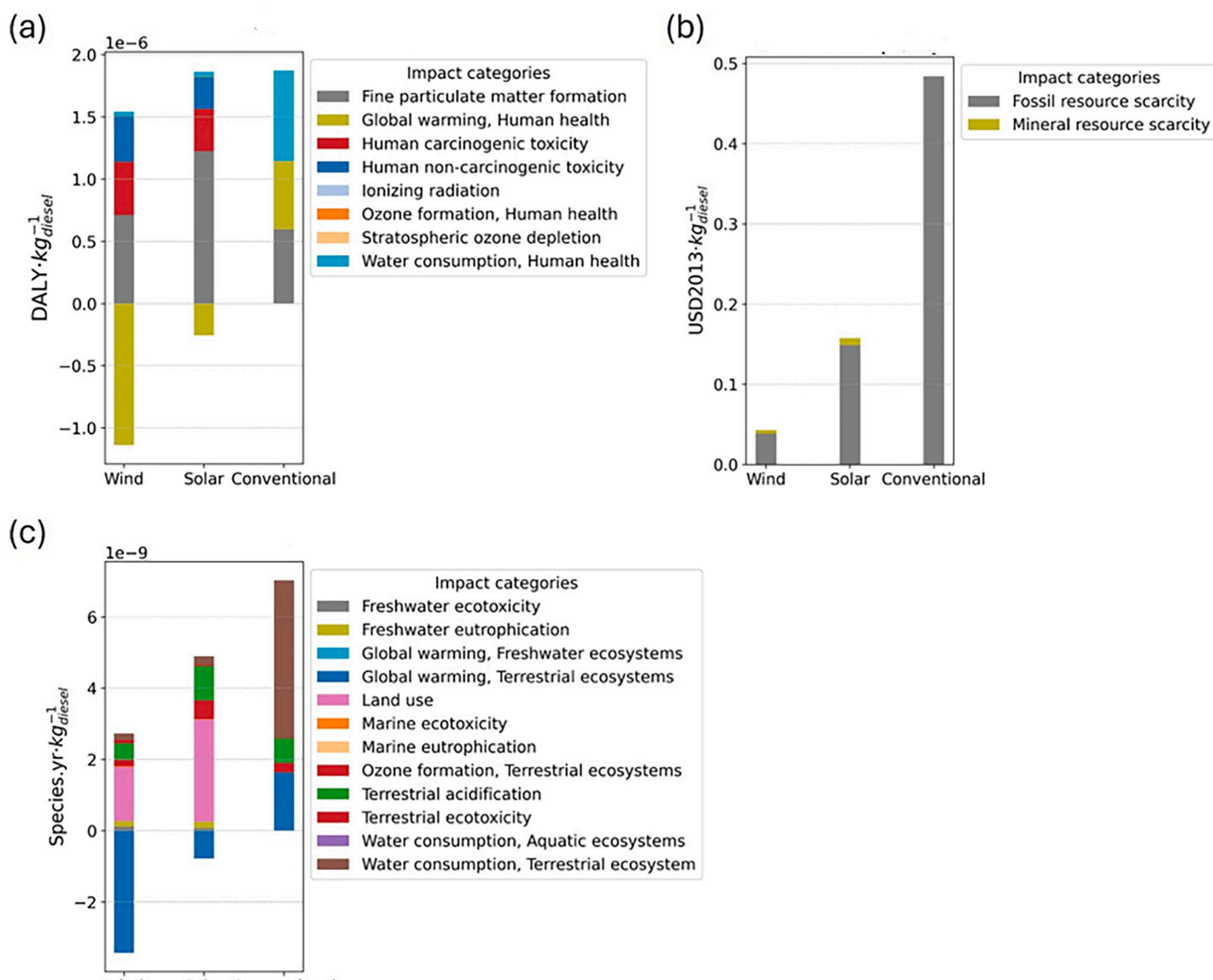

Fig. 4. Results for the endpoint impact categories for the integrated process at the nominal case study and a comparison with the BAU: A) Human health, B) Resources, C) Ecosystem quality.

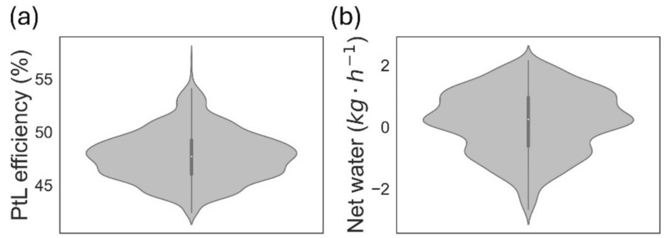

Fig. 5. Uncertainty analysis results for the (a) power-to-liquid efficiency, and (b) the net water consumption. The central black bar in each plot represents the interquartile range, with a white dot indicating the median. Black lines extending from this bar mark the lower and upper adjacent values, with any points beyond these lines considered outliers. (PtL = Power to Liquid).

not conventional process, electricity mostly affects each term contributing to total human health while cooling water also affects the water consumption, human health.

Resource values for the BAU system, integrated process using solar and wind energy are respectively 0.48 USD2013/kg_{diesel}, 0.15 USD2013/kg_{diesel} and 0.04 USD2013/kg_{diesel}. Electricity has the highest impact on resources for the proposed integrated process.

On the other hand, the ecosystem quality of the BAU system, integrated process using solar and wind energy is respectively of $7.02 \bullet 10^{-9}$ species·yr/kg_{diesel}, $4.12 \bullet 10^{-9}$ species·yr/kg_{diesel} and $-7.1 \bullet 10^{-9}$ species·yr/kg_{diesel}. Also in this impact category, electricity is the greater contributor followed by sorbent production (for climate change, freshwater ecosystems and climate change, terrestrial ecosystems) and cooling water (water consumption, aquatic ecosystems and water consumption, terrestrial ecosystem).

It is clear that for the endpoint impact categories, electricity consumption mostly dictates the overall environmental performance. As for the midpoint impact categories, a comparison with the literature cannot be conducted for the endpoint impact categories because it has not been investigated in the literature yet.

3.2. Results for the GSA

Violin plots in Figs. 5 and 6 depict the total variance of the output metrics when all critical uncertain parameters are simultaneously varied. Figs. 7 and 8 showcase the explained variance through the GSA by presenting the total-order sensitivity indices for all KPIs. Values of these indices are reported in Tables S10 and S11 of the supplementary information (Section 4).

It should be noted that no input-input interactions are observed for any of the KPIs (i.e. second-order indices are 0), and therefore the model exhibits an additive structure. The monitored KPIs are technoeconomic (overall power-to-liquid efficiency, net amount of water inside the plant, production cost) and environmental (midpoint and endpoint impact categories). The KPIs for the heat closed loop is not considered in the GSA due to the complex pinch analysis even though the nominal case study shows the potentiality of plant for this aspect.

Factors with a value of total-order Sobol indices higher than 5 % are considered significant for the KPI under investigation (Zhang et al., 2015). According to this assumption, significant factors for the overall PtL efficiency variability (42.2 %–57 % as the interquartile range) as shown in Fig. 5a, are the electrical efficiency the voltage efficiency of the alkaline cell, (both related to the electrical energy consumption of the electrolytic cell) and CO recycle ratio in the FT synthesis. These factors account for 50 %, 30.3 %, and 19.5 % for the variability of the PtL efficiency, respectively (Fig. 7). In fact, the electrical consumption will

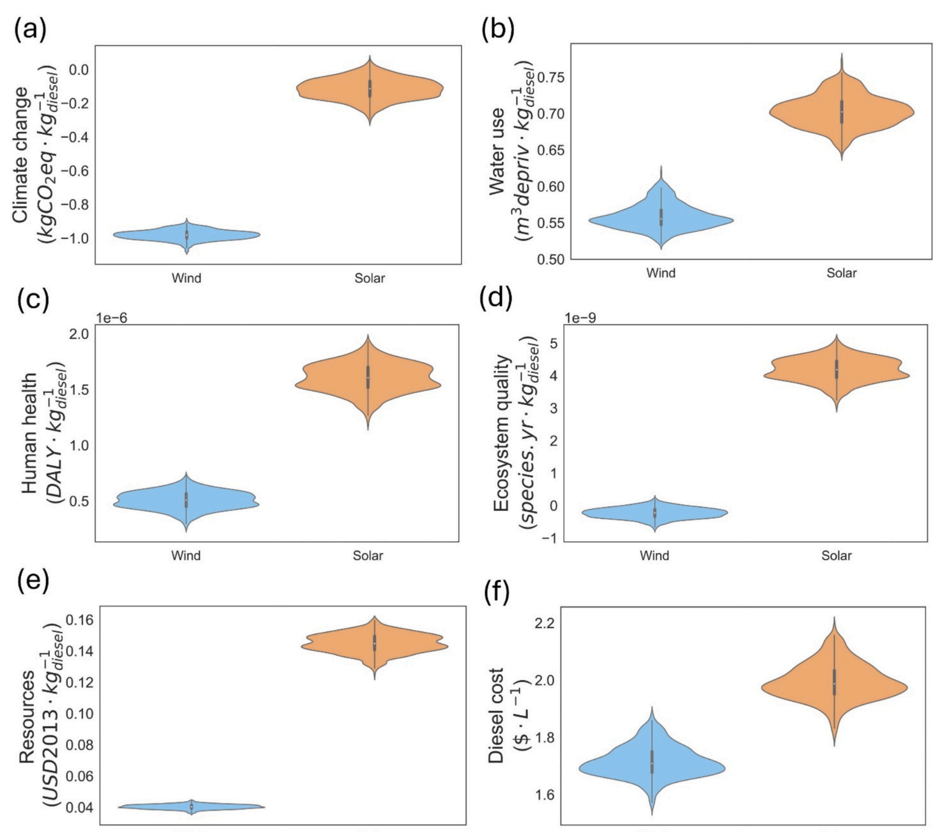

Fig. 6. Uncertainty analysis results for (a) climate change, (b) water use, (c) human health, (d) ecosystem quality, and (e) diesel production cost, for wind and solar energy. The central black bar in each plot represents the interquartile range, with a white dot indicating the median. Black lines extending from this bar mark the lower and upper adjacent values, with any points beyond these lines considered outliers.

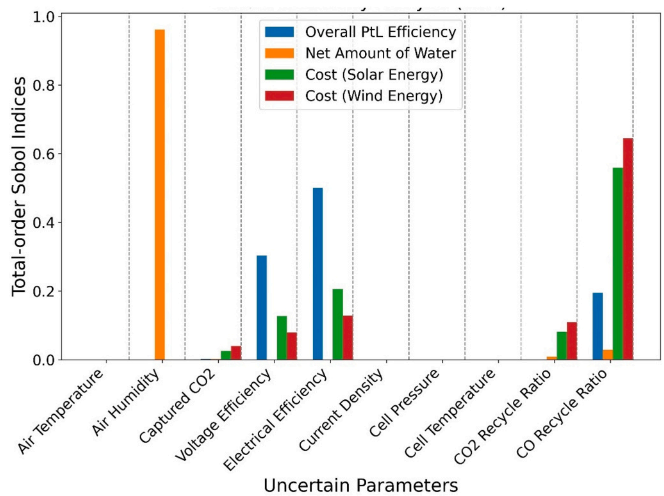

Fig. 7. Total-order Sobol indices for PtL efficiency, diesel production cost and net amount of water inside the plant. (PtL = power-to-liquid).

affect the denominator of the efficiency correlation while the CO recycle ratio will affect the numerator of the same formula through the amount of produced fuel.

The net amount of water in the integrated process varies between −2.67 kg/h to 2.14 kg/h with a median value of 0.25 kg/h, which is very close to closing the water loop as seen in Fig. 5. Only air humidity, determining the amount of water captured in DAC, is significant for the net amount of water inside the process by accounting for 96.1 % of its variability (Fig. 7).

The variance of the levelized cost of diesel is attributed to the same parameters for both solar and wind energy routes (Fig. 6f), which are the CO recycle ratio, voltage efficiency, electrical efficiency, and amount of captured CO_2. The major contributor to the levelized cost uncertainty is the CO recycle ratio, which accounts for 64.4 % of the variability when the fuel is produced with wind energy and 55.9 % when solar energy is used. The different percentage is due to a higher cost of electricity production from solar energy causing a higher influence of voltage efficiency and electrical efficiency inputs when interactions are negligible. The electrical efficiency follows by contributing to 20.6 % and 12.8 % of the variability when solar and wind energy is used, respectively (Fig. 7).

The above results suggest that costs and power-to-liquid efficiency are independent of the geographic location of the plant (air humidity and temperature are not significant); however, this is not the case for the metrics of the net amount of heat and water. It is important to find the optimal weather conditions in order to have a closed loop for water and heat.

Among midpoint impact categories, water use and climate change are considered. Air humidity, voltage efficiency and electrical efficiency are significant for water use when both solar and wind energies are used for the electrical energy (Fig. 8). This is in agreement with the previous result: the water loop is strongly dependent on the geographic location. Specifically, air humidity accounts for 66 % and 42.8 % of the water use variability for wind and solar, respectively. Following air humidity, the electrical efficiency affects more the fuel produced by solar (32.4 %) compared to wind (17.8 %) energy. On the other hand, for climate change, when solar energy is driving the process, air humidity, voltage efficiency, electrical efficiency, CO recycle ratio have important effects on the considered response. When wind energy is driving the process, air temperature and CO_2 recycle ratio also influence the process (Fig. 8). It is also observed that there is less uncertainty (i.e. variability) for the climate change impact when wind energy is used, compared to solar energy (Fig. 6a). As for water use, the climate change impact is also dependent on the location of the plant.

Among endpoint impact categories, human health, resources and ecosystem quality are taken into account. Voltage efficiency, electrical efficiency and CO recycle ratio are significant for human health when both solar and wind energy are used (Fig. 8). In terms of impact on resources, there is almost no uncertainty in this metric for fuel derived from wind energy (Fig. 6e). On the other hand, the variability of the resources for the solar energy fuel is mostly attributed to the electrical efficiency (56.3 %), the voltage efficiency of alkaline cell (35.1 %), and the CO recycle ratio (8.5 %) (Fig. 8). For the ecosystem quality, the voltage efficiency of alkaline cell, electrical efficiency and CO recycle ratio have an important effect when solar energy is used. When wind energy is driving the process, air humidity and temperature also slightly affect that endpoint impact category (Fig. 8).

Overall, almost all of the endpoint impact categories do not depend on the geographic location of the plant, in contrast to the midpoint impact categories evaluated here.

Moreover, these results show that for climate change, ecosystem quality and resources impacts, different inputs are significant when solar and wind energy are used to produce electrical energy although the

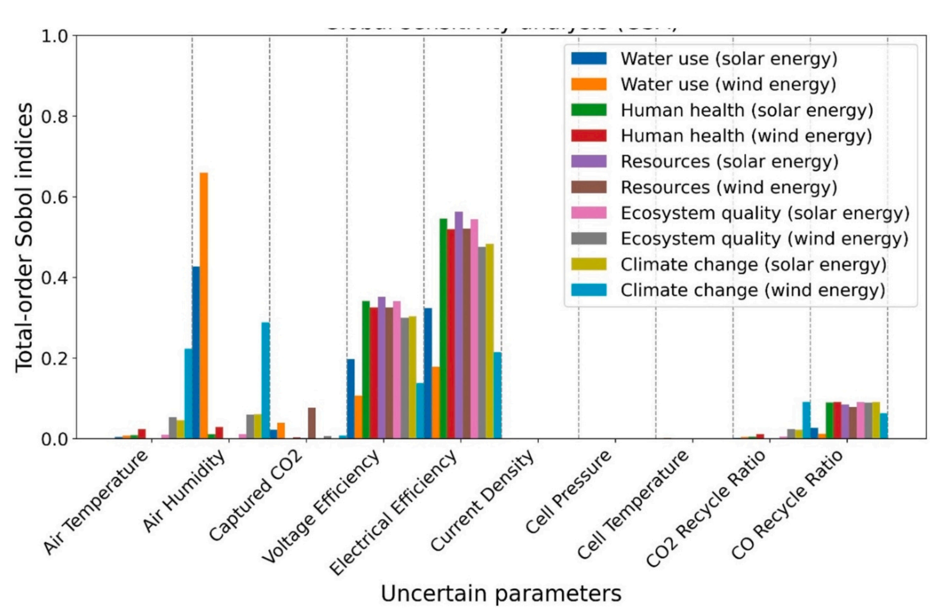

Fig. 8. Total-order Sobol indices for midpoint and endpoint impact categories.

voltage efficiency of electrolysers and electrical efficiency have an important effect in all these responses. Considering that voltage efficiency and electrical efficiency are influencing the electricity consumption, the obtained result is due to the different environmental impacts of electricity production from solar and wind energy. In particular, the production of electricity by solar energy has an environmental impact on climate change, ecosystem quality and resources higher compared to that obtained by wind energy. Moreover, the electricity production from solar energy has a higher impact on those impact categories compared to that of the electricity production from wind energy and the electricity production from solar energy contributes more than 90 % on the discussed impact categories. This causes, for voltage efficiency and electrical efficiency inputs, a higher value of total order Sobol index. The sum of total order Sobol index is limited to one (because no significant interactions are present) so that a lower number of potential significant inputs are present, when solar energy is used, in comparison to the case when wind energy is exploited.

4. Conclusions

A new process scheme to produce diesel from CO_2 via FT synthesis is proposed here and characterized by a desire to ensure, as far as possible, circularity of water, CO_2 and heat. In particular, the CO_2 captured from the air through an adsorption-based system is used for fuel production while water from the reaction synthesis and DAC is fed to the alkaline electrolytic cell and heat for DAC regeneration is coming from the FT synthesis, boiler and electrolytic cell.

Through material and energy balances of the proposed process, it is verified that with an overall PtL efficiency of 43.5 % and a diesel production cost of 1.76 $\$/liter_{diesel}$ and 2.07 $\$/liter_{diesel}$ when wind and solar energy are used, CO_2, water and heat closed loops are ensured.

However, a full LCA shows that a perfect closed loop is not present for the water use and a further optimization of water consumption/production inside the overall process is needed from an environmental point of view.

Then a global sensitivity analysis is conducted to attribute the variability of KPIs to specific uncertain process parameters.

It is found that even though costs and efficiency are independent of the geographic location (e.g. air temperature and humidity) this is not the case for midpoint impact categories for which optimal weather conditions and hence locations should be identified.

As an additional result, the most important input in a PtL process is the electrical energy consumption in the electrolytic cell so that the combination of a higher efficiency of electrolytic cell with the optimal weather conditions can ensure a PtL process producing diesel characterized by circularity in CO_2, water and heat and with a production cost that could be comparable with that of the market.

CRediT authorship contribution statement

Grazia Leonzio: Writing – original draft, Software, Methodology, Investigation, Funding acquisition, Formal analysis, Data curation, Conceptualization. **Niki Triantafyllou:** Software, Data curation, Conceptualization, Writing – review & editing. **Nilay Shah:** Writing – review & editing, Supervision, Conceptualization.

Acknowledgments

The authors would like to thank the University of Cagliari and Imperial College London.

Appendix A. Supplementary data

Supplementary data to this article can be found online at https://doi.org/10.1016/j.spc.2024.09.018.

References

Adelung, S., 2022. Global sensitivity and uncertainty analysis of a Fischer-Tropsch based power-to-liquid process. Journal of CO2 Utilization 65, 102171.
Adelung, S., Maier, S., Dietrich, R.U., 2021. Impact of the reverse water-gas shift operating conditions on the power-to-liquid process efficiency. Sustain Energy Technol Assess 43, 100897.
Ahamed, A., Veksha, A., Yin, K., Weerachanchai, P., Giannis, A., Lisak, G., 2020. Environmental impact assessment of converting flexible packaging plastic waste to pyrolysis oil and multi-walled carbon nanotubes. J. Hazard. Mater. 390, 121449.
Ahamed, A., Vallam, P., Iyer, N.S., Veksha, A., Bobacka, J., Lisak, G., 2021. Life cycle assessment of plastic grocery bags and their alternatives in cities with confined waste management structure: a Singapore case study. J. Clean. Prod. 278, 123956.
Becker, W.L., Braun, R.J., Penev, M., Melaina, M., 2012. Production of FischereTropsch liquid fuels from high temperature solid oxide co-electrolysis units. Energy 47, 99–115.
Berticelli, R., Pandolfo, A., Reichert, G.A., Salazar, R.F.D.S., Kalil, R.M., 2020. Support system for decision-making processes related to municipal solid waste management by taking into consideration a sustainable life cycle assessment: review on environmental, economic and social aspects. Int. J. Environ. Waste Manag. 26 (2), 147–167.
Bertuccioli, L., Chan, A., Hart, D., Lehner, F., Madden, B., Standen, E., 2014. Study on development of water electrolysis in the EU. In: E4tech Report.
Bisotti, F., Hoff, K.A., Mathisen, A., Hovland, J., 2024. Direct air capture (DAC) deployment: a review of the industrial deployment. Chem. Eng. Sci. 283, 119416.
Brauns, J., Turek, T., 2020. Alkaline water electrolysis powered by renewable energy: a review. Processes 8 (2), 248.
Buffo, G., Ferrero, D., Santarelli, M., Lanzini, A., 2020. Energy and environmental analysis of a flexible power-to-X plant based on reversible solid oxide cells (rSOCs) for an urban district. J. Energy Storage 29 (2020), 101314.
Calemma, V., Gambaro, C., Parker, W.O., Carbone, R., Giardino, R., Scorletti, P., 2010. Middle distillates from hydrocracking of FT waxes: composition, characteristics and emission properties. Catal. Today 149 (1–2), 40–46.
Climeworks, 2020. Available at www.climeworks.com (Accessed on July 2020).
Cucurachi, S., Borgonovo, E., Heijungs, R., 2016. A protocol for the global sensitivity analysis of impact assessment models in life cycle assessment. Risk Anal. 36, 357–377.
Dahiya, S., Katakojwala, R., Ramakrishna, S., Mohan, S.V., 2020. Biobased products and life cycle assessment in the context of circular economy and sustainability. Mat. Circ. Econ. 2 (1), 1–28.
Dieterich, V., Buttler, A., Hanel, A., Spliethoff, H., Fendt, S., 2020. Power-to-liquid via synthesis of methanol, DME or Fischer–Tropsch-fuels: a review. Energ. Environ. Sci. 13 (10), 3207–3252.
EIA, 2023. Energy and the environment explained: greenhouse gases and the climate. Available from: https://www.eia.gov/about/.
El-Halwagi, M.M., 2017. Sustainable Design Through Process Integration: Fundamentals and Applications to Industrial Pollution Prevention, Resource Conservation, and Profitability Enhancement. Butterworth-Heinemann.
European Commission, 2018. A clean planet for all - a European long-term strategic vision for a prosperous, modern, competitive and climate neutral economy. Eur. Comm. 114. https://ec.europa.eu/clima/sites/clima/files/docs/pages/com_2018_733_en.pdf?utm_campaign=AktuellHållbarhet-Direkten_181129_Username&utm_medium=email&utm_source=Eloqua&elqTrackId.
Falter, C., Batteiger, V., Sizmann, A., 2016. Climate impact and economic feasibility of solar thermochemical jet fuel production. Environ. Sci. Technol. 50, 470–477.
Fasihi, M., Bogdanov, D., Breyer, C., 2016. Techno-economic assessment of power-to-liquids (PtL) fuels production and global trading based on hybrid PV-wind power plants. Energy Procedia 99, 243–268.
Foolmaun, R.K., Ramjeawon, T., 2013. Life cycle sustainability assessments (LCSA) of four disposal scenarios for used polyethylene terephthalate (PET) bottles in Mauritius. Environ. Dev. Sustain. 15 (3), 783–806.
Fratalocchi, L., Visconti, C.G., Groppi, G., Lietti, L., Tronconi, E., 2018. Intensifying heat transfer in Fischer-Tropsch tubular reactors through the adoption of conductive packed foams. Chem. Eng. J. 349, 829–837.
Freire Ordonez, D., Shah, N., Guillen-Gosalbez, G., 2021. Economic and full environmental assessment of electrofuels via electrolysis and co-electrolysis considering externalities. Appl. Energy 286, 116488.
Freire Ordonez, D., Halfdanarson, T., Ganzer, C., Shah, N., Mac Dowellac, N., Guillen-Gosalbez, G., 2022. Evaluation of the potential use of e-fuels in the European aviation sector: a comprehensive economic and environmental assessment including externalities. Sustainable Energy Fuels 6, 4749.
Garcıa-Valverde, R., Espinosa, N., Urbina, A., 2012. Simple PEM water electrolyser model and experimental validation. Int. J. Hydrogen Energy 37, 1927–1938.
GlobalPetrolPrice, 2024. Available at: https://www.globalpetrolprices.com/diesel_prices/.
Groen, E.A., Bokkers, E.A.M., Heijungs, R., de Boer, I.J.M., 2017. Methods for global sensitivity analysis in life cycle assessment. Int. J. Life Cycle Assess. 22, 1125–1137.
Heidgen, K., Maas, H., Hombach, L.E., Dor, L., Wallington, T.J., Walther, G., 2019. Economic and Environmental Assessment of Current (2015) and Future (2030) Use of E-fuels in Light-duty Vehicles in Germany, 207, pp. 153–162.
Herz, G., Rix, C., Jacobasch, E., Müller, N., Reichelt, E., Jahn, M., Michaelis, A., 2021. Economic assessment of power-to-liquid processes – influence of electrolysis technology and operating conditions. Appl. Energy 292 (2021), 116655.
Hillestad, M., 2015. Modeling the Fischer-Tropsch product distribution and model implementation. Chem. Prod. Process. Model. 10 (3), 147–159.

HPV, 2009. Available at: https://www.petroleumhpv.org/petroleum-substances-and-categories/~/media/9540e567ae1a4d69833de465eccf3d02.ashx.
Hu, S., Guo, B., Ding, S., Yang, F., Dang, J., Liu, B., Gu, J., Ma, J., Ouyang, M., 2022. A comprehensive review of alkaline water electrolysis mathematical modeling. Appl. Energy 327, 120099.
Intratec, 2024. available at: https://www.intratec.us/products/water-utility-costs/commodity/cooling-water-cost.
IPCC, 2018. An IPCC special report on the impacts of global warming of 1.5 °C above pre-industrial levels and related global greenhouse gas emission pathways, in the context of strengthening the global response to the threat of climate change, sustainable development, and efforts to eradicate poverty. In: Masson-Delmotte, V., Zhai, P., Portner, H.-O., Roberts, D., Skea, J., Shukla, P.R., Pirani, A., Moufouma-Okia, W., P'ean, C., Pidcock, R., Connors, S., Matthews, J.B.R., Chen, Y., Zhou, X., Gomis, M.I., Lonnoy, E., Maycock, T., Tignor, M., Watereld, T. (Eds.), Global Warming of 1.5 °C. World Meteorological Organization, Geneva, Switzerland.
IRENA, 2020. Green Hydrogen Cost Reduction: Scaling up Electrolysers to Meet the 1.5°C Climate Goal. International Renewable Energy Agency, Abu Dhabi.
Isaacs, S.A., Staples, M.D., Allroggen, F., Mallapragada, D.S., Falter, C.P., Barrett, S.R.H., 2021. Environmental and economic performance of hybrid power-to-liquid and biomass-to-liquid fuel production in the United States. Environ. Sci. Technol. 55, 8247–8257.
ISO 14040, 2009. Environmental Management – Life Cycle Assessment – Principles and Framework. European Committee for Standardisation, Brussels.
ISO 14044, 2006. Environmental Management – Life Cycle Assessment – Requirements and Guidelines. European Committee for Standardisation, Brussels.
Kang, J., Ma, W., Keogh, R.A., Shafer, W.D., Jacobs, G., Davis, B.H., 2012. Hydrocracking and Hydroisomerization of n-Hexadecane, n-Octacosane and Fischer–Tropsch Wax Over a Pt/SiO2–Al2O3 Catalyst. Catal. Lett. 142, 1295–1305.
Kim, D.H., Park, J.L., Park, E.J., Kim, Y.D., Uhm, S., 2014. Dopant effect of barium zirconatebased perovskite-type catalysts for the intermediate-temperature reverse water gas shift reaction. ACS Catal. 4, 3117–3122.
Konig, D.H., Baucks, N., Dietrich, R.U., Worner, A., 2015a. Simulation and evaluation of a process concept for the generation of synthetic fuel from CO2 and H2. Energy 91, 833–841.
Konig, D.H., Freiberg, M., Dietrich, R.U., Wörner, A., 2015b. Techno-economic study of the storage of fluctuating renewable energy in liquid hydrocarbons. Fuel 159, 289–297.
Kucherenko, S., 2013. SOBOLHDMR: a general-purpose modeling software. Methods Mol. Biol. 1073, 191–224.
Kucherenko, S., Song, S., 2017. Different numerical estimators for main effect global sensitivity indices. Reliab. Eng. Syst. Saf. 165, 222–238.
Larson, E.D., Jin, H., Celik, F.E., 2005. Gasification-based Fuels and Electricity Production from Biomass, without and with Carbon Capture and Storage. Princeton University, Princeton.
Lee, J., Hwang, S., Seo, J.G., Lee, S.B., Jung, J.C., Song, I.K., 2010. Production of middle distillate through hydrocracking of paraffin wax over Pd/SiO2–Al2O3 catalysts. J. Ind. Eng. Chem. 16, 790–794.
Lehtonen, J., Jarnefelt, V., Alakurtti, S., Arasto, A., Hannula, I., Harlin, A., Koljonen, T., Lantto, R., Lienemann, M., Onarheim, K., Pitkanen, J.P., Tahtinen, M., 2019. The Carbon Reuse Economy: Transforming CO2 From a Pollutant into a Resource. VTT Tech. Res. Cent. Finl.
Leonzio, G., 2024. Life cycle assessment of carbon dioxide supply chains: state of the art and methodology description. Appl. Sci. 14, 385.
Leonzio, G., Fennell, P.S., Shah, N., 2022a. A comparative study of different sorbents in the context of direct air capture (DAC): evaluation of key performance indicators and comparisons. Appl. Sci. 12, 2618.
Leonzio, G., Mwabonje, O., Fennell, P.S., Shah, N., 2022b. Environmental performance of different sorbents used for direct air capture. Sustainable Production and Consumption 32, 101–111.
Leonzio, G., Bogle, I.D.L., Foscolo, P.U., 2023a. Life cycle assessment of a carbon capture utilization and storage supply chain in Italy and Germany: comparison between carbon dioxide storage and utilization systems. Sustainable Energy Technologies and Assessment 55, 102743.
Leonzio, G., Chachuat, B., Shah, N., 2023b. Towards ethylene production from carbon dioxide: economic and global warming potential assessment. Sustainable Production and Consumption 43, 124–139.
Liu, C.M., Sandhu, N.K., McCoy, S.T., Bergerson, J.A., 2020. A life cycle assessment of greenhouse gas emissions from direct air capture and Fischer–Tropsch fuel production. Sustainable Energy Fuels 4, 3129.
Llatas, C., Soust-Verdaguer, B., Passer, A., 2020. Implementing life cycle sustainability assessment during design stages in building information modelling: from systematic literature review to a methodological approach. Build. Environ. 182, 107164.
Marchese, M., Giglio, E., Santarelli, M., Lanzini, A., 2020. Energy performance of power-to-liquid applications integrating biogas upgrading, reverse water gas shift, solid oxide electrolysis and Fischer-Tropsch technologies. Energ. Conver. Manage. 6, 100041.
Marchese, M., Buffo, G., Santarelli, M., Lanzini, A., 2021. CO2 from direct air capture as carbon feedstock for Fischer-Tropsch chemicals and fuels. Energy and economic analysis, Journal of CO2 Utilization 46, 101487.
Marion, M.C., Bertoncini, F., Hugues, F., Forestiere, A., 2006. Comprehensive Characterisation of Products from Cobalt Catalysed FischerTropsch Reaction, DGMK/SCI-Conference "Synthesis Gas Chemistry", October 4–6, 2006, Dresden, Germany.
Martín, M., Grossmann, I.E., 2011. Process optimization of FT diesel production from lignocellulosic switchgrass. Ind. Eng. Chem. Res. 50, 13485–13499.
Medrano-García, J.D., Charalambous, M.A., Guillén-Gosálbez, G., 2022. Economic and environmental barriers of CO2-based Fischer−Tropsch electro-diesel. ACS Sustainable Chem. Eng. 10, 11751–11759.
Mertens, J., Breyer, C., Arning, K., Bardow, A., Belmans, R., Dibenedetto, A., Erkman, S., Gripekoven, J., Léonard, G., Nizou, S., Pant, D., Reis-Machado, A.S., Styring, P., Vente, J., Webber, M., Sapart, C.J., 2023. Carbon capture and utilization: more than hiding CO2 for some time. Joule 7 (3), 442–449.
Micheli, M., Moore, D., Bach, V., Finkbeiner, M., 2022. Life-cycle assessment of power-to-liquid kerosene produced from renewable electricity and CO2 from direct air capture in Germany. Sustainability 14, 10658.
OurworldIndata, 2023. available at: https://ourworldindata.org/co2-and-greenhouse-gas-emissions#all-charts.
OurWorldInData, 2024. Available at: https://ourworldindata.org/grapher/levelized-cost-of-energy?country=~USA.
Peters, R., Wegener, N., Samsun, R.C., Schorn, F., Riese, J., Grünewald, M., Stolten, D., 2022. A Techno-Economic Assessment of Fischer–Tropsch Fuels Based on Syngas from Co-Electrolysis. Processes 10, 699.
Repasky, J.M., Zeller, R.L., 2021. Process for the Conversion of Carbon Dioxide (WO2021062384A1).
Rivera-Tinoco, R., Farran, M., Bouallou, C., Aupretre, F., Valentin, S., Millet, P., et al., 2016. Investigation of power-to-methanol processes coupling electrolytic hydrogen production and catalytic CO2 reduction. Int. J. Hydrogen Energy 41 (8), 4546–4559.
Rojas-Michaga, M.F., Michailos, S., Cardozo, E., Akram, M., Hughes, K.J., Ingham, D., Pourkashanian, M., 2023. Sustainable aviation fuel (SAF) production through power-to-liquid (PtL): a combined techno-economic and life cycle assessment. Energ. Conver. Manage. 292, 117427.
Sadhukhan, J., Gadkari, S., Martinez-Hernandez, E., Ng, K.S., Shemfe, M., TorresGarcia, E., Lynch, J., 2019. Novel macroalgae (seaweed) biorefinery systems for integrated chemical, protein, salt, nutrient and mineral extractions and environmental protection by green synthesis and life cycle sustainability assessments. Green Chem. 21 (10), 2635–2655.
Saltelli, A., Annoni, P., Azzini, I., Campolongo, F., Ratto, M., Tarantola, S., 2010. Variance based sensitivity analysis of model output. Design and estimator for the total sensitivity index. Comput. Phys. Commun. 181, 259–270.
Samavati, M., Martin, A., Santarelli, M., Nemanova, V., 2018. Synthetic diesel production as a form of renewable energy storage. Energies 11, 1223.
Sandeep, K.C., Kamath, S., Mistry, K., Kumar, M.A., Bhattacharya, S.K., Bhanja, K., Mohan, S., 2017. Experimental studies and modeling of advanced alkaline water electrolyser with porous nickel electrodes for hydrogen production. Int. J. Hydrogen Energy 42, 12094–12103.
Schemme, S., Samsun, R.C., Peters, R., Stolten, D., 2017. Power-to-fuel as a key to sustainable transport systems–an analysis of diesel fuels produced from CO2 and renewable electricity. Fuel 205, 198–221.
Schmidt, P., 2016. Weindorf W. Power-to-Liquids: Potentials and Perspectives for the Future Supply of Renewable Aviation Fuel (Dessau-Roßlau; September:1–36).
Schmidt, P., Batteiger, V., Roth, A., Weindorf, W., Raksha, T., 2018. Power-to-liquids as renewable fuel option for aviation: a review. Chem. Ing. Tech. 2018 (90), 1–2 (127–140).
Sendi, M., Bui, M., Mac Dowell, N., Fennell, P., 2022. Geospatial analysis of regional climate impacts to accelerate cost-efficient direct air capture deployment. One Earth 5, 1153–1164.
Smith, R., 2005. Chemical Process Design and Integration. McGraw Hill Editor.
Sobol, I.M., 2001. Global Sensitivity Indices for Nonlinear Mathematical Models and Their Monte Carlo Estimates.
Soler, A., Gordillo, V., Lilley, W., Schmidt, P., Werner, W., Houghton, T., Dell'Orco, S., 2022. E-fuels: a techno-economic assessment of European domestic production and imports towards 2050. In: Concawe and Aramco Report No. 17/22.
Spath, P., Aden, A., Eggeman, T., Ringer, M., Wallace, B., Jechura, J., 2005. Biomass to hydrogen production detailed design and economics utilizing the Battelle Columbus Laboratory indirectly-heated gasifier. In: Technical Report: NREL/TP510-37408.
Sphera, 2022. available at: https://sphera.com/wp-content/uploads/2022/02/Introduction-to-Water-Use-Assessment-in-GaBi-2022.pdf.
Stamford, L., 2020. Life cycle sustainability assessment in the energy sector. In: Biofuels for a More Sustainable Future, pp. 115–163 vols.
TESARRECTM Trademark: UK00003321198. available at: https://tesarrec.web.app/sustainability.
Toweringskills, 2024. Available at: https://toweringskills.com/financial-analysis/cost-indices/.
Verdegaal, W., Becker, S., von Olshausen, C., 2015. Power-to-liquid: synthetisches Rohol aus CO2, Wasser und Sonne. Chem. Ing. Tech. 87, 340e6.
Yoo, E., Lee, U., Zang, G., Sun, P., Elgowainy, A., Wang, M., 2022. Incremental approach for the life-cycle greenhouse gas analysis of carbon capture and utilization. Journal of CO2 Utilization 65, 102212.
Zang, G., Sun, P., Elgowainy, A.A., Bafana, A., Wang, M., 2021. Performance and cost analysis of liquid fuel production from H2 and CO2 based on the Fischer-Tropsch process. Journal of CO2 Utilization 46, 101459.
Zhang, X.Y., Trame, M.N., Lesko, L.J., Schmidt, S., 2015. Sobol sensitivity analysis: a tool to guide the development and evaluation of systems pharmacology models. CPT Pharmacometrics Syst. Pharmacol. 4 (2), 69–79.
Zhang, X., Zhang, L., Fung, K.Y., Bakshi, B.R., Ng, K.M., 2020. Sustainable product design: a life-cycle approach. Chem. Eng. Sci. 217, 115508.
Zhou, Y., Searle, S., Pavlenko, N., 2022. Current and future cost of e-kerosene in the United States and Europe, ICCT WORKING PAPER 2022-14. https://theicct.org/wp-content/uploads/2022/02/fuels-us-europe-current-future-cost-ekerosene-us-europe-mar22.pdf.